



Asymmetric flow field flow fractionation of aqueous C₆₀ nanoparticles with size determination by dynamic light scattering and quantification by liquid chromatography atmospheric pressure photo-ionization mass spectrometry

Carl W. Isaacson^a, Dermont Bouchard^{b,*}

^a National Research Council Research Associate, Athens, GA, USA

^b Environmental Protection Agency, National Exposure Research Laboratory, 960 College Station Road, Athens, GA 30606, USA

ARTICLE INFO

Article history:

Received 21 September 2009

Received in revised form

11 December 2009

Accepted 22 December 2009

Available online 4 January 2010

Keywords:

Asymmetric flow field flow fractionation (AF4)

Fullerene

Nanoparticle

C60

ABSTRACT

A size separation method was developed for aqueous C₆₀ fullerene aggregates (aqu/C₆₀) using asymmetric flow field flow fractionation (AF4) coupled to a dynamic light scattering detector in flow through mode. Surfactants, which are commonly used in AF4, were avoided as they may alter suspension characteristics. Aqu/C₆₀ aggregates generated by sonication in deionized water ranged in size from 80 to 260 nm in hydrodynamic diameter (D_h) as determined by DLS in flow through mode, which was corroborated by analysis of fractions by DLS in batch mode and by TEM. The mass of C₆₀ in each fraction was determined by LC-APPI-MS. Only $5.2 \pm 6.7\%$ of the total aqu/C₆₀ mass had D_h less than 80 nm, while $58 \pm 32\%$ of the total aqu/C₆₀ mass had D_h between 80 and 150 nm and $14 \pm 9.2\%$ of the total aqu/C₆₀ were between 150 and 260 nm in D_h . With the optimal fractionation parameters, $77 \pm 5.8\%$ of the aqu/C₆₀ mass eluted from the AF4 channel, indicating deposition on the AF4 membrane had occurred during fractionation; use of alternative membranes did not reduce deposition. Channel flow splitting increased detector response although channel split ratios greater than 80% of the channel flow led to decreased detector response. This is the first report on the use of AF4 for fractionating a colloidal suspension of aqu/C₆₀.

Published by Elsevier B.V.

1. Introduction

There is a growing interest in the use of fullerene nanomaterials in electronic, biomedical and photovoltaic applications [1–3]. As these materials enter into industrial and consumer use, it is inevitable that they will become dispersed in the environment. Therefore, it is essential that the risk these materials may pose to human and environmental health be determined [4,5]. This research need has led many scientists to report on the formation of suspensions of nanometer size fullerene aggregates [6–8], and the toxicity [8–11], environmental behavior and transport of these aggregates [12,13]. However, the lack of specific analytical methods for the detection and quantification of aggregated fullerene nanomaterials in environmental systems greatly limits these studies [4,5]. Analytical methods need to be developed which can size separate materials in the nanometer range, while providing specific detection which allows for the differentiation between engineered and naturally occurring nanometer sized materials [4,5].

Current methods employed to determine the fullerene aggregate size distributions of aqueous C₆₀ suspensions (aqu/C₆₀)

include transmission electron microscopy (TEM), atomic force microscopy (AFM), and light scattering (e.g. dynamic and static light scattering, DLS and SLS, respectively) [6–8,13–16]. TEM and AFM are not well suited for the analysis of large numbers of samples and cannot be used to determine the molecular composition of materials [17]. While light scattering techniques are applicable to large numbers of samples, light scattering techniques too cannot be used to determine molecular composition of analytes [17]. To date, methods for the size separation of fullerene suspensions utilize filtration [6–8,13–16,18] and centrifugation [14] that may introduce contaminants into the sample matrix and do not provide direct information on aggregate size-distribution. Size exclusion chromatography (SEC) was successful in separating fullerene complexes [19–21], but is limited to narrow aggregate size ranges, the upper size limit of SEC columns (approximately 10⁶ molecular weight), shear degradation and extensive analyte-matrix interactions of separation in packed columns [22].

Asymmetric flow field flow fractionation (AF4) is an open channel size fractionation technique in which particles are separated based on differences in diffusion coefficients [23–25]. AF4 is a versatile method for separating aggregates ranging in size from 1 to 500 nm in normal mode and under a range of elution solvent conditions [23,25]. This versatility with respect to mobile phase composition allows for the use of deionized water or aqueous buffer

* Corresponding author. Tel.: +1 706 355 8333.

E-mail address: bouchard.dermont@epa.gov (D. Bouchard).

solutions with ionic strengths as high as 10 mM [23] without the addition of other mobile phase modifiers, such as surfactants, that will affect aggregate size and surface charge. The ability to utilize a wide array of aqueous mobile phase conditions allows AF4 separations to be conducted under the same background solution conditions in which the suspensions are generated.

By size-separating polydisperse aggregates with AF4 prior to size determination by light scattering, the occlusion of small aggregates by larger aggregates and the subsequent lack of resolution between aggregate populations is ameliorated [26]. This fractionation is advantageous as the fundamental limitation of light scattering detectors is the scattered light intensity dependence on aggregate size in polydisperse samples [26], which results in the poor resolution of light scattering detectors for polydisperse samples. Additionally, ultraviolet detectors and refractive index detectors are often coupled to AF4s to detect and quantify analytes [23], but these detectors do not provide sufficient specificity to unambiguously quantify C₆₀ [17]. However, if fractions of the AF4 eluent are collected and the mass of aqu/C₆₀ in each fraction is quantified by liquid chromatography–atmospheric pressure photoionization–mass spectrometry (LC–APPI–MS), unambiguous determinations of the mass of C₆₀ in each size fraction are achieved [17].

Reported herein are the first methods for the AF4 size separation of aqu/C₆₀ aggregates in deionized water without the use of mobile phase modifiers coupled with in-line dynamic light scattering (DLS) and off-line with LC–APPI–MS. Initial investigations were aimed at determining optimal cross flow rates to achieve optimal size separation. The DLS size determinations in flow through mode were supported with batch mode DLS measurements and TEM analysis of the AF4 fractions. Experiments were also conducted to determine how AF4 membrane type and injection volume affect the aqueous fullerene size separation. In addition, experiments aimed at enhancing detector response through split channel flow were conducted.

2. Experimental

2.1. Materials

Standards of C₆₀ (>99%) and ¹³C₆₀ (>99% C₆₀ with 20–30% enriched in ¹³C) were purchased from MER Corp., Tuscon, AZ. Toluene and methanol (HPLC grade) were purchased from Sigma–Aldrich (St. Louis, MO).

2.2. Aqu/C₆₀ suspension preparation

Fullerene suspensions were generated without the use of organic solvents by high power sonication in water. Briefly, 25 mg of pre-ground C₆₀ powder was added to 50 mL of deionized water (resistivity > 18 MΩ/cm), sonicated in an ultrasonic processor (GENEQ, Montreal, QC), delivering 300 W for 5 min, allowed to cool for 5 min, and sonicated at the same power for another 5 min. The aqu/C₆₀ suspensions were filtered with 0.45 μm cellulose acetate filters (Chrom Tech Inc., Apple Valley, MN).

2.3. Asymmetric flow field flow fractionation (AF4) coupled with in-line dynamic light scattering detection

An AF4 (Postnova, Salt Lake City Utah) with deionized water eluent was coupled in flow through mode to a DLS detector (Zetasizer NanoZS, Malvern, Westborough, MA). The trapezoidal AF4 channel was 27.5 cm long from tip to tip with tapered inlets and outlets. The tapered inlet and outlet were 4 and 1 cm long, respectively, with base widths of 2 and 0.5 cm, respectively. The fractionations were accomplished with a 350 μm spacer and initially with a 500 μL

injection loop, subsequent experiments were conducted with 50, 100, 1000 or 2000 μL injection loops. The AF4 was initially outfitted with a 10 kDa polyethersulfone membrane (Postnova Salt Lake City Utah). Additional experiments were conducted with a Celgard 2320 polypropylene membrane, 30 nm pore size (Charlotte, NC), a 10 kDa regenerated cellulose membrane (Postnova Salt Lake City Utah), and a 10 nm pore size polycarbonate membrane (GE Water and Process Technologies, Minnetonka, MN), each of which were exchanged each day.

The AF4 elution program consisted of a 2–15 min injection and focusing period, depending on the injection volume, in which the tip flow was 0.2 mL/min, and the cross flow was set to 1, 2 or 4 mL/min. The focusing flow, only used during the sample injection period, is set by the AF4 software to equal the sum of the cross flow and detector flow less the tip flow. The detector flow was set to 1 mL/min for all fractions, except for fractionations conducted with outlet stream splitting. For fractionations with outlet stream splitting, the sum of the outlet stream flow and the detector flow were 1 mL/min. The injection and focusing program was followed by the elution program in which the cross flow was held constant for 2 min at the same flow rate as the focusing step and then decreased non-linearly over the next 10 min. The non-linear cross flow gradient is described by the equation [27]:

$$V_x(t) = V_{x,i} - \frac{V_{x,i} - V_{x,f}}{(t_f - t_i)^n} (t - t_i)^n \quad (1)$$

where $V_x(t)$ is the cross flow at a given time t , $V_{x,i}$ is the initial cross flow, $V_{x,f}$ is the final cross flow, t_f is the time at which the gradient ends, t_i is the time at which the gradient begins and n determines the rate at which the cross flow decreases, in the present study $n=0.05$. The cross flow gradient was followed by a 2 min period in which the cross flow was set to 0 mL/min. The size of the fractionated aggregates was measured by DLS in flow through mode.

In batch and flow through mode the DLS correlates fluctuations in photons scattered by particles with time. The diffusion coefficient is calculated from this correlation by the cumulant method. The intensity weighted hydrodynamic size, D_h , is then calculated from the diffusion coefficient via the Stokes–Einstein Equation. The D_h is a single, intensity-weighted value representing the entire aggregate size distribution in a three second time increment.

2.4. Characterization of AF4 fractions with LC–APPI–MS and TEM

A combination of two previously published methods were used to quantify C₆₀ [9,28]. Aqu/C₆₀ was extracted into toluene following destabilization of the colloidal suspension with NaCl and quantified with ¹³C₆₀ internal standard calibration by liquid chromatography atmospheric pressure photo-ionization mass spectrometry (LC–APPI–MS).

Separation of C₆₀ was performed on an Accela liquid chromatograph (LC), Thermo Fisher (West Palm Beach, FL). The LC was outfitted with a cosmosil (150 mm × 4 mm) column connected inline to a 3 mm × 4 mm guard column (Phenomenex, Torrance, CA) with a 95% toluene 5% methanol mobile phase. The LC was connected to a Quantum Ultra triple quadrupole mass spectrometer (MS), Thermo Fisher (West Palm Beach, FL). The MS was operated in negative APPI mode with N₂ vaporization gas, a source temperature of 450 °C and with the krypton photoionization lamp operating at 10 eV. The MS was set to select molecular ions C₆₀ (m/z 720) and ¹³C₆₀ (m/z 734) as precursor and product ion in multiple reaction monitoring mode as no fragments or adducts were observed which would increase analytical specificity [9,28].

For TEM imaging aqu/C₆₀ suspensions were drop deposited on a 200 mesh Formvar coated copper grid. The images were acquired at 300 kV on a Hitachi-9500 TEM with a 2K Gatan CCD camera or at

120 kV on a Hitachi 7600 TEM with a 1 K Gatan CCD camera, each with an exposure time of 1 s.

3. Results and discussion

3.1. Optimizing elution program

The initial unfractionated aqu/C₆₀ suspension aggregates had a hydrodynamic diameter (D_h) of 130 ± 1 nm, a polydispersity index of 0.16, a zeta potential (ζ) of -40 ± 1 mV, and a C₆₀ mass concentration of 1.7 ± 0.12 mg/L. For this suspension, the predicted elution time estimation program of Leeman et al. [29] indicates that a non-linear gradient with an exponent of 0.05 (from Eq. (1)) is needed to resolve aqu/C₆₀ aggregates into size classes. Use of exponents greater than 0.05 are predicted to result in decreased resolution over the 10–300 nm aqu/C₆₀ aggregate size range, while exponents less than 0.05 will not result in increased resolution over the size range of interest. Therefore, an elution gradient with an exponent of 0.05 was selected for the separation of aqu/C₆₀ aggregates.

At an initial cross flow of 1 mL/min and a channel flow of 1 mL/min, aqu/C₆₀ aggregates were retained from the void time of the channel and size separated (Fig. 1A). During elution, aqu/C₆₀ aggregates continuously increased in size with the smallest detected aqu/C₆₀ aggregates having a D_h of 110 nm and the largest aqu/C₆₀ aggregates having a D_h of 200 nm (Fig. 1A). The

observation of elution of smaller aggregates followed by elution of larger aggregates is consistent with normal mode AF4 separation theory [23]. The apparent lower cutoff of 110 nm results from the lack of resolution of smaller aqu/C₆₀ aggregates at a cross flow of 1 mL/min: aggregates less than 110 nm in D_h are occluded from size determination by coelution with the 110 nm D_h aqu/C₆₀ (Fig. 1A).

The observation of 110 nm D_h aqu/C₆₀ eluting at 7.8 min is in poor agreement with the predicted retention time of 11.7 min ($RT_{\text{calculated}}/RT_{\text{measured}} = 1.5$); however, the agreement improved with increasing aggregate size as 200 nm D_h aqu/C₆₀ eluted at 12 min versus a predicted retention time of 13.4 min ($RT_{\text{calculated}}/RT_{text{measured}} = 1.1$) (Table 1). Early elution, relative to the predicted elution time, was observed for all size separations and was previously reported for low ionic strength eluents [30–32]. Early elution results from repulsive electrostatic interactions between analytes and the membrane, resulting in lower particle concentrations at the accumulation membrane surface [30–32]. The improving agreement between predicted and measured retention times with increasing aggregate size may result from the larger aggregates being immobilized against the accumulation membrane at the beginning of the fractionation and therefore eluting relatively later [29]. Conventionally, the size of fractionated particles is determined from the observed retention time; however, this method of size determination is greatly complicated by the non-ideal retention of aqu/C₆₀ aggregates. This problem is circum-

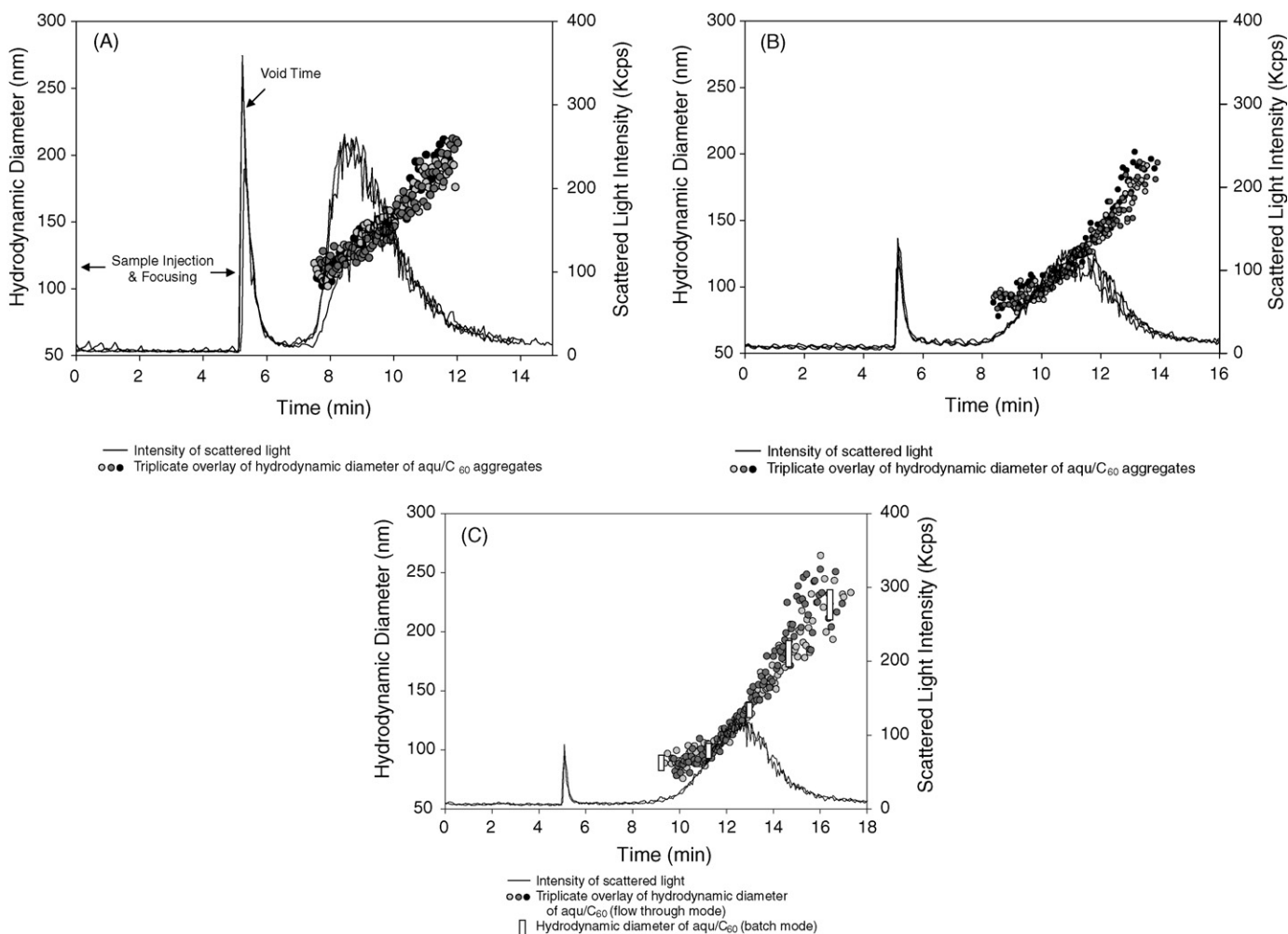


Fig. 1. (A–C) Fractograms of aqu/C₆₀ showing intensity of scattered light and aqu/C₆₀ aggregate size distributions with initial cross flow rates of 1 mL/min (A), 2 mL/min (B) and 4 mL/min (C). The sample is injected and focused in the AF4 channel in the first 5 min followed by elution of un-retained analytes at the 5 min void time. Retained analytes elute in order of increasing size from 7.5 to 18 min.

Table 1Observed and calculated retention times for aqu/C₆₀.

Particle size (nm)	RT _{observed} (min) ($\pm 95\%$ CI)	RT _{calculated} (min)	RT _{Calculated} /RT _{Observed}
110	7.8 \pm 0.2	11.5	1.5
125	8.5 \pm 0.1	11.8	1.4
150	9.9 \pm 0.3	12.3	1.3
175	10.9 \pm 0.4	12.8	1.2
200	12.0 \pm 0.6	13.2	1.1

vented by size determining the aggregates with a light scattering detector post-AF4 separation.

3.2. Optimizing cross flow

With a cross flow of 1 mL/min and a channel flow of 1 mL/min, $4.2 \pm 1.8\%$ (average of $n=3$, $\pm 95\%$ confidence interval (CI)) of the injected aqu/C₆₀, eluted in the void time of the channel (Fig. 2A), and therefore was not included in further mass distribution calculations. The mass of aqu/C₆₀ in the 6–8 min fraction was $9.1 \pm 1.3\%$ of the injected aqu/C₆₀ mass and these aggregates were less than 110 nm in D_h (Figs. 1A and 2A). The 110–150 nm aqu/C₆₀, which eluted from 8 to 10 min, accounted for $50 \pm 32\%$ of the injected mass (Fig. 2A), which is consistent with the batch measurement of 129 ± 1 nm for the un-fractionated aqu/C₆₀. The mass of aqu/C₆₀ eluting in the subsequent 10–12 min fraction accounted for $12 \pm 18\%$ of the injected mass and ranged in size from 150

to 200 nm in D_h (Figs. 1A and 2A). The 12–16 min fractions contained $5.0 \pm 9.6\%$ of the aqu/C₆₀; however, the aggregates were not sufficiently resolved to permit size determination by DLS (Figs. 1 and 2A).

Of the aqu/C₆₀ aggregates that were fractionated by AF4 at a cross flow of 1 mL/min, $76 \pm 7.5\%$ eluted from the AF4 indicating that aqu/C₆₀ was deposited in the AF4 channel during fractionation (Fig. 2A). This deposition was further corroborated by the appearance of a brown residue in the focusing area of the AF4 membrane after repeated injection of aqu/C₆₀. Additionally, aqu/C₆₀ did not pass through the membrane in appreciable amounts as the cross flow eluent contained less than 1% of the injected aqu-C₆₀ mass. Deposition is unexpected as the aqu/C₆₀ aggregates have a ζ of -40 ± 1 mV and polyethersulfone (PES) membranes have an isoelectric point of pH 3.1 [33]. Therefore, repulsive interactions are expected between the aqu/C₆₀ and the PES membrane. Deposition during the focusing period likely results from the

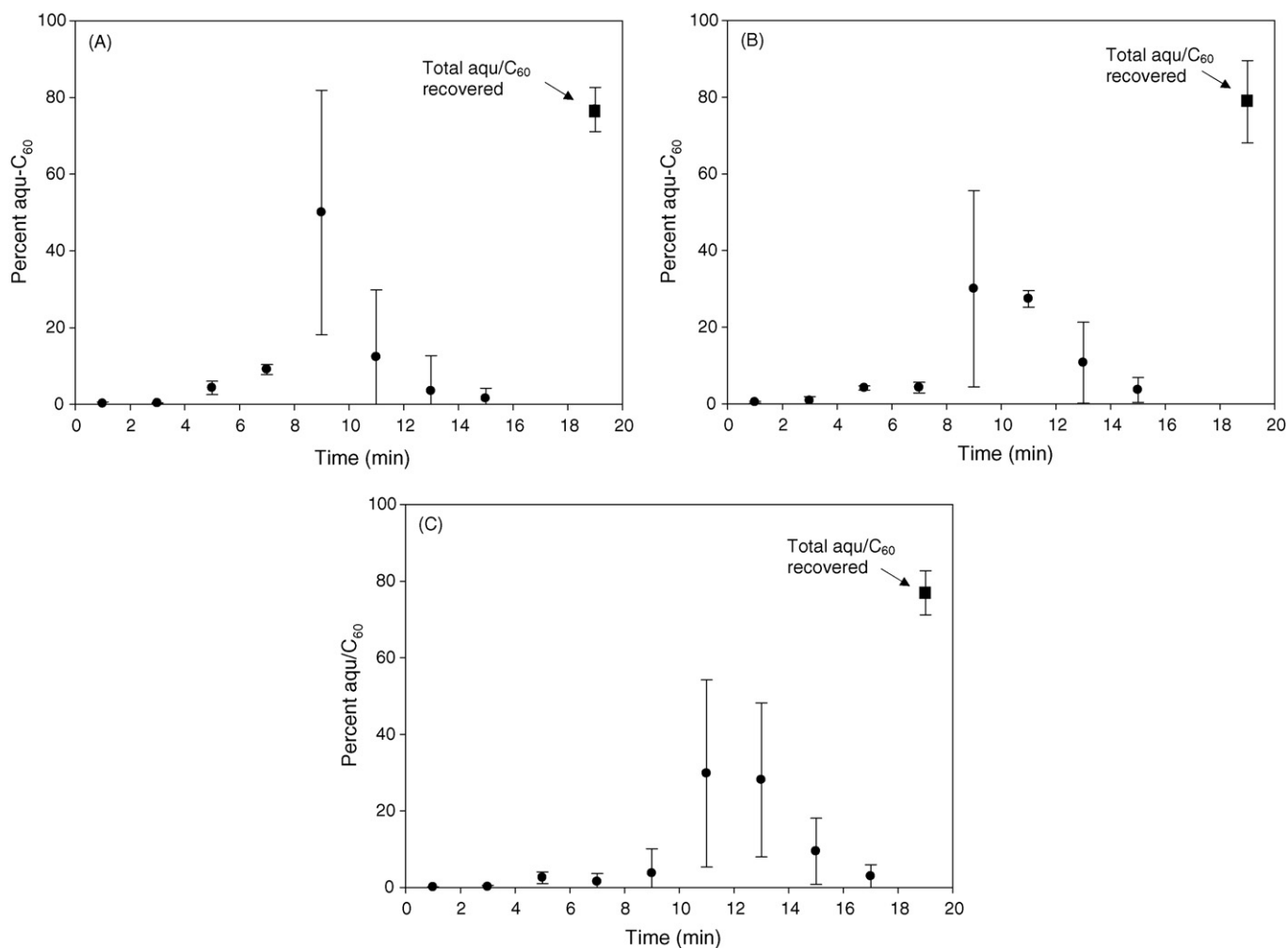


Fig. 2. (A–C) Means and 95% CIs for mass analysis of AF4 fractograms with cross flow rates of 1 mL/min (A), 2 mL/min (B) and 4 mL/min (C) fractions collected in 2 min intervals (●), total aqu/C₆₀ recovered (■).

increased particle-membrane interactions that occur during the sample focusing.

When the cross flow was increased to 2 mL/min and the channel flow was kept constant at 1 mL/min, aqu/C₆₀ ranged in size from 80 to 200 nm in D_h (Fig. 2A). The observation of smaller D_h aggregates with fractionation programs at increased cross flow is consistent with AF4 theory [23]. Of the injected aqu/C₆₀, $4.1 \pm 0.5\%$ of the aqu/C₆₀ eluted in the 4–6 min fraction, the void time of the channel, which is statistically equivalent to the mass eluted in the void volume at 1 mL/min (Fig. 2A and B). Aggregates less than 80 nm in diameter accounted for $4.2 \pm 1.4\%$ of the injected mass of aqu/C₆₀, as determined from the mass collected in the 6–8 min fraction (Figs. 1B and 2B). The 80–100 nm (8–10 min fraction) and 100–130 nm aggregates (10–12 min fraction) comprised 30 ± 26 and $27 \pm 2.1\%$ of the injected C₆₀ mass, respectively (Fig. 1B and 2B). The aqu/C₆₀ aggregates in the 12–16 min fractions ranged in size from 130 to 200 nm in D_h and accounted for $14 \pm 11\%$ of the aqu/C₆₀ mass (Figs. 1B and 2B). The mass of aqu/C₆₀ that eluted from the channel, $76 \pm 14\%$, was not statistically different than the mass eluted at a cross flow of 1 mL/min (Fig. 2A and B). When compared to the fractionation obtained with a cross flow of 1 mL/min, the cross flow of 2 mL/min provided improved retention and separation which allowed for the detection of aggregates down to 80 nm in D_h .

When the cross flow was increased further to 4 mL/min and the channel flow was maintained at 1 mL/min, aqu/C₆₀ aggregates ranged in size from 80 to 260 nm D_h (Fig. 1C), which is consistent with higher cross flows allowing greater resolution for smaller aggregates [29]. Observing the same lower cutoff of 80 nm D_h with a cross flows of 2 and 4 mL/min indicates that 80 nm aggregates are the smallest aqu/C₆₀ aggregates present in sufficient concentration to permit size determination by DLS. While the difference in the mass of aqu/C₆₀ eluting at the void time for the 4 mL/min cross flow is not statistically significant from other fractionation programs, there is a trend of reduced elution at the void time of the channel with increasing cross flow rates (Fig. 2A–C), which is consistent with AF4 theory [25]. At a cross flow of 4 mL/min, $5.2 \pm 6.7\%$ of the aqu/C₆₀ had D_h less than 80 nm, which is in good agreement with the $4.2 \pm 1.4\%$ observed with a cross flow of 2 mL/min (Fig. 2B and C). Aqu/C₆₀ with 80–100 nm D_h eluted in the 10–12 min fraction and accounted for $30 \pm 24\%$ of the injected aqu/C₆₀ mass (Fig. 1C and 2C), in good agreement with the $30 \pm 26\%$ measured at 2 mL/min cross flow rate for the same size fraction (Figs. 1B and 2B). Aqu/C₆₀ with D_h ranging from 100 to 150 nm eluted from 12 to 14 min and comprised $28 \pm 20\%$ of the injected aqu/C₆₀ mass (Figs. 1C and 2C). Aqu/C₆₀ aggregates eluting in the 14–18 min fraction ranged in size from 150 to 260 nm in D_h , and accounted for $14 \pm 9.2\%$ of the aqu/C₆₀ (Figs. 1C and 2C). The use of a fractionation program with an initial cross flow of 4 mL/min resulted in elution of $77 \pm 5.8\%$ of the mass of the injected aqu/C₆₀, indicating that a cross flow of 4 mL/min does not result in increased deposition on the membrane when compared to cross flows of 1 and 2 mL/min (Fig. 2A–C).

3.3. Optimizing detector response through outlet stream splitting

Outlet stream splitting is possible because the cross flow forces analytes into the 1–10 μm region closest to the accumulation membrane leaving most of the channel void of analytes [25]. By splitting the channel flow into two streams and only passing the flow stream containing analytes through the detector, the detector response is increased. If the analytes are in the 1–10 μm closest to the membrane [25], optimum outlet stream splitting will result in splitting more than 95% of the eluent to waste and 5% of the eluent to the detector, potentially increasing detector response by a factor of 20.

When the outlet split flow was increased from 50% to 80% of the channel flow, the detector response increased by a factors of 1.3

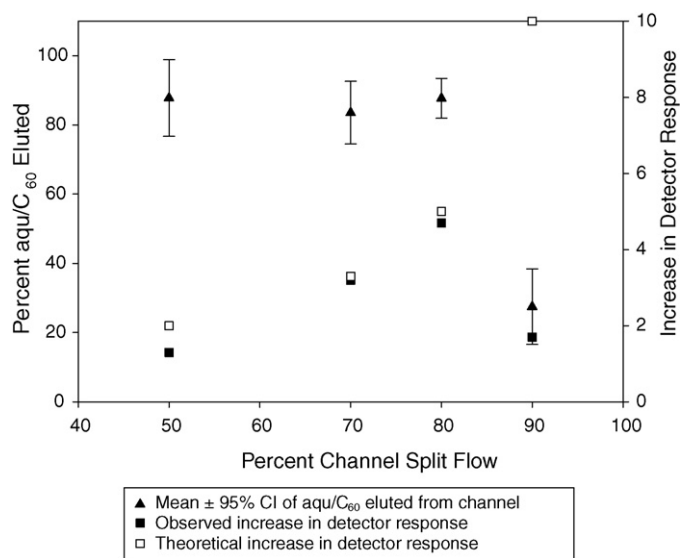


Fig. 3. Elution of aqu/C₆₀ and increase in detector response as a function of channel split flow.

to 4.7, respectively (Fig. 3). This increase in detector response is in good agreement with the predicted increase in detector response by factors of 2–5. Additionally, the percentage of aqu/C₆₀ eluting through the detector remained constant (Fig. 3), indicating that analyte was not being lost in the split. When the outlet stream split was further increased to 90% of the channel flow only $28 \pm 11\%$ of the injected aqu/C₆₀ eluted through the detector, and the detector response increased by a factor of 1.7, rather than the predicted increase of 10 (Fig. 3). The low recovery and detector response using 90% split indicates that there is non-ideal flow in the channel resulting in loss of aqu/C₆₀ through the outlet waste flow. Therefore, the optimal split flow is 80%, as compared to the theoretic optimum of 95% [25].

3.4. Confirmation of aggregate size

To confirm the size determinations made by DLS in flow through mode, size determinations of the fractions were conducted with DLS in batch mode and by TEM. The batch DLS measurements were in excellent agreement with the flow through measurements (Fig. 1C), validating the use of DLS inline with AF4. The batch DLS measurements commonly used to characterize these systems usually rely on a single average D_h value and a measure of polydispersity to represent the entire particle size distribution. While this approach is adequate for relatively homogeneous colloidal suspensions, it becomes less informative for more heterogeneous suspensions likely to be encountered in environmental samples. AF4 coupled with DLS and LC–APPI–MS is able to fractionate aqu/C₆₀ suspensions to determine the particle mass in each particle size class.

Size determinations by TEM of the 100–150 nm fraction, the most concentrated fraction, were in general agreement with the size determinations by DLS (Fig. 4A). For fractions larger and smaller than 100–150 nm, the dilute particle concentration and aggregation of aqu/C₆₀ during sample preparation greatly reduced confidence in size determinations by TEM (Fig. 4B–D).

3.5. Effects of membrane type and increasing injection volume on deposition

To reduce deposition in the AF4 channel during fractionation, membranes of different chemistries and pore sizes including,

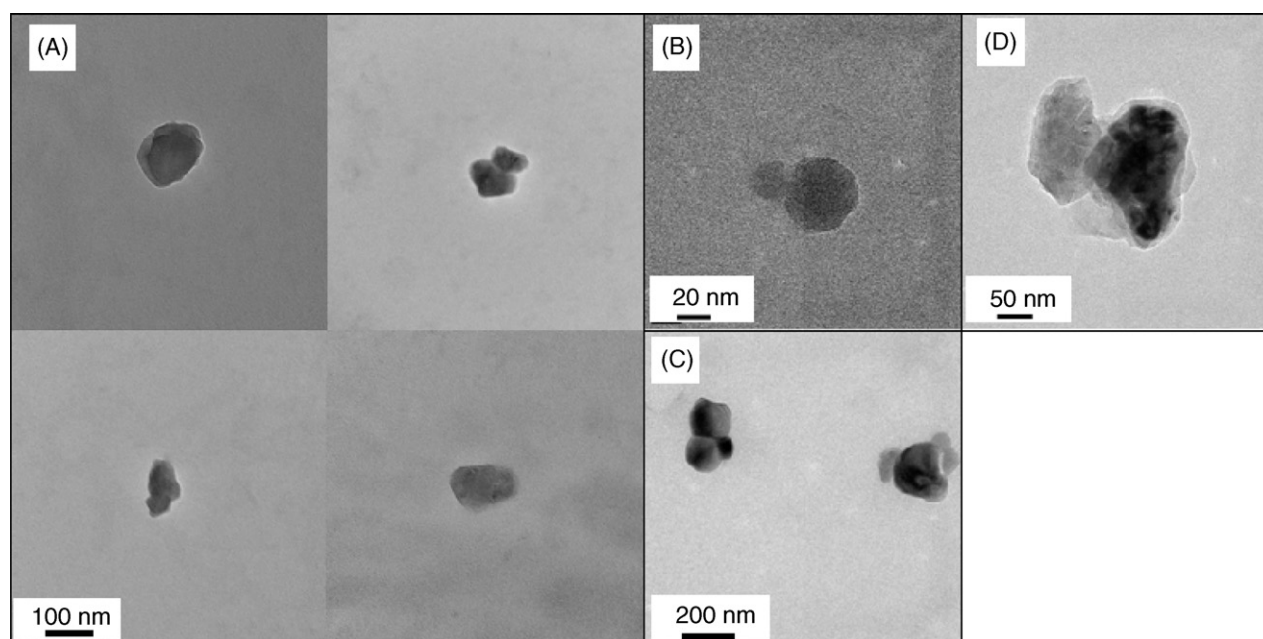


Fig. 4. (A–D) TEM images of aqu/C₆₀ fractionated with an initial cross flow of 4 mL/min: 100–150 nm D_h aggregates (A), 80–100 nm D_h aggregates (B), 150–200 nm D_h aggregates (C), and (D) 200–260 nm D_h aggregates.

10 kDa polyethersulfone (PES), 10 kDa cellulose acetate, 10 nm pore size polycarbonate and 30 nm pore size polypropylene membranes were investigated. Additionally, injection volumes of 50, 100, 500, 1000, and 2000 μ Ls were evaluated to determine if the mass of aqu/C₆₀ fractionated effects the amount of deposition.

The percent of aqu/C₆₀ eluted from the AF4 channel was statistically equivalent for the 10 kDa PES, 10 kDa cellulose acetate, and 30 nm polypropylene membranes (Table 2), indicating that membrane aromaticity, electron donating capacity, hydrophobicity, and pore size do not determine aqu/C₆₀ deposition. However, only $29 \pm 5.1\%$ of the injected aqu/C₆₀ eluted from the AF4 channel when a 10 nm pore size polycarbonate membrane was used (Table 2). As polycarbonate and PES membranes are chemically similar (both have aromatic and electron donating functionality) and have similar isoelectric points (Table 2) the increased deposition on the polycarbonate membrane does not result from different membrane chemistries. Additionally, the decreased elution observed with the polycarbonate membrane does not result from the 10 nm pore size as the 30 nm pore size polypropylene membrane had little deposition. Therefore, the low recovery observed with the polycarbonate membrane is likely due to surface heterogeneities on the membrane which retained aqu/C₆₀.

To determine how the mass of aqu/C₆₀ injected effects the deposition of aqu/C₆₀, fractionations were conducted using 50, 100, 500, 1000, 2000 μ L injections of aqu/C₆₀ suspension. With small injection volumes of 50 and 100 μ L only $33 \pm 5.0\%$ and $67 \pm 7.0\%$ of

the aqu/C₆₀ eluted from the AF4 (Fig. 5). When the injection volume was increased to 500, 1000, and 2000 μ L the percent of the aqu/C₆₀ that eluted from the AF4 increased to $77 \pm 5.8\%$, $87 \pm 3.3\%$ and $89 \pm 5.8\%$, respectively (Fig. 5). Obtaining low recoveries at low injection volumes and higher recoveries at higher injection volumes indicates that there are a limited number of sorption sites for aqu/C₆₀ in the AF4 channel. In the present study, 500- μ L injection volumes were used to minimize deposition during fractionation.

3.6. Environmental analytical applications of this study

The polydisperse nature of aqu/C₆₀ suspensions with respect to particle size is problematic for size characterization of these suspensions, but is also problematic for colloidal transport studies, toxicity studies, and other environmental studies with aqu/C₆₀ or other particulate species where size is an important variable. The AF4 methodologies described above provide for improved particle size characterization through fractionation followed by size determination by DLS and mass determination by mass spectrometry.

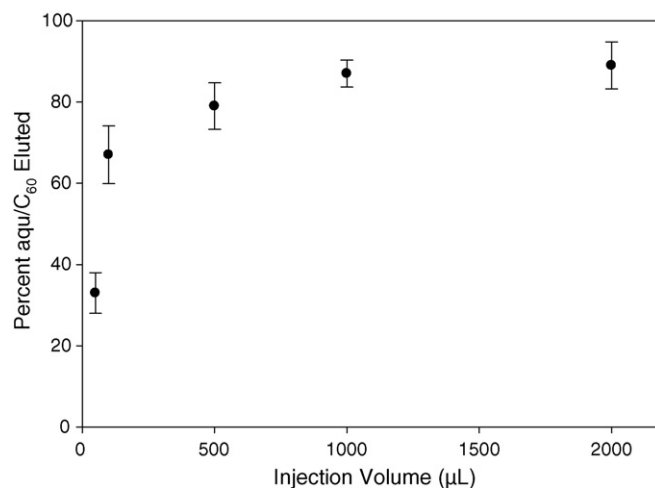


Fig. 5. Mean and 95% CIs for elution of aqu/C₆₀ as a function of injection volume.

Table 2

Recovery of aqu/C₆₀ during AF4 separation when using different membranes.

Membrane type	Recovery ($\pm 95\%$ CI)	IEP ^a	Pore size
Polyethersulfone	$79 \pm 5.7\%$	3.1 ^b	10 kDa ^c
Cellulose Acetate	$73 \pm 7.7\%$	4.2 ^b	10 kDa ^c
Polypropylene	$75 \pm 5.3\%$	4 ^d	30 nm ^c
Polycarbonate	$29 \pm 5.1\%$	3 ^e	10 nm ^c

^a Isoelectric point (IEP).

^b Pontie et al. [33].

^c As per manufactures specification.

^d Stakne et al. [34].

^e Nagel et al. [35].

In addition, since the fractionation method is non-destructive and can be performed under a wide range of background solution conditions, aqu/C₆₀ fractions with narrower size distributions can be generated for further study in transport, toxicity, or other studies.

Disclaimer

This paper has been reviewed in accordance with the U.S. Environmental Protection Agency's peer and administrative review policies and approved for publication. Mention of trade names or commercial products does not constitute endorsement or recommendation for use.

Acknowledgements

The authors would like to acknowledge Jean-Luc Brousseau (Malvern Instruments) and Soheyl Tadjiki (Postnova Analytics) for their helpful insights, Haijun Qian (Clemson Electron Microscopy Facility) for his help in collecting TEM images and Susan Richardson (EPA, Athens, GA) for the use of the LC–APPI–MS. The authors would also like to thank Sung Gung Lee, Xin (Cissy) Ma, Bethany Wigington, and Tiantiana Burns for the assistance and good humor they provided over the course of this study.

References

- [1] D.M. Guldi, N. Martin, Fullerenes: From Synthesis to Optoelectronic Properties, Kluwer Academic Publishers, 2002.
- [2] Woodrow Wilson International Center for Scholars, Project on Emerging Nanotechnologies, 2007.
- [3] N. Tagmatarchis, H. Shinohara, Mini-Rev. Med. Chem. 1 (4) (2001) 339.
- [4] The National Nanotechnology Initiative, Environmental, Health, and Safety Research Needs for Engineered Nanoscale Materials, 2006.
- [5] USEPA, U.S. Environmental Protection Agency, Nanotechnology White Paper, 2007.
- [6] X. Ma, D. Bouchard, Environ. Sci. Technol. 43 (2) (2008) 330.
- [7] S. Deguchi, R.G. Alargova, K. Tsujii, Langmuir 17 (19) (2001) 6013.
- [8] J.D. Fortner, D.Y. Lyon, C.M. Sayes, A.M. Boyd, J.C. Falkner, E.M. Hotze, L.B. Alemany, Y.J. Tao, W. Guo, K.D. Ausman, V.L. Colvin, J.B. Hughes, Environ. Sci. Technol. 39 (11) (2005) 4307.
- [9] C.W. Isaacson, C.Y. Usenko, R.L. Tanguay, J.A. Field, Anal. Chem. 79 (23) (2007) 9091.
- [10] C.Y. Usenko, S.L. Harper, R.L. Tanguay, Carbon 45 (9) (2007) 1891.
- [11] E. Oberdorster, Environ. Health Perspect. 112 (2004) 1058.
- [12] Y. Li, Y. Wang, K.D. Pennell, L.M. Abriola, Environ. Sci. Technol. 42 (19) (2008) 7174.
- [13] J. Brant, H. Lecoanet, M. Hotze, M. Wiesner, Environ. Sci. Technol. 39 (17) (2005) 6343.
- [14] D.Y. Lyon, L.K. Adams, J.C. Falkner, P.J.J. Alvarez, Environ. Sci. Technol. 40 (12) (2006) 4360.
- [15] J.A. Brant, J. Labille, J.Y. Bottero, M.R. Wiesner, Langmuir 22 (8) (2006) 3878.
- [16] A. Dhawan, J.S. Taurozzi, A.K. Pandey, W. Shan, S.M. Miller, S.A. Hashsham, V.V. Tarabara, Environ. Sci. Technol. 40 (23) (2006) 7394.
- [17] C.W. Isaacson, M. Kleber, J.A. Field, Environ. Sci. Technol. 43 (17) (2009) 6463.
- [18] L.K. Duncan, J.R. Jinschek, P.J. Vikesland, Environ. Sci. Technol. 42 (1) (2008) 173–178.
- [19] K.L. Wooley, C.J. Hawker, J.M.J. Frechet, F. Wudl, G. Srdanov, S. Shi, C. Li, M. Kao, J. Am. Chem. Soc. 115 (1993) 9836.
- [20] A.M. Ramos, M.T. Rispens, J.K.J. van Duren, J.C. Hummelen, R.A.J. Janssen, J. Am. Chem. Soc. 123 (2001) 6714.
- [21] B. Belgorodsky, L. Fadeev, J. Kolsenik, M. Gozin, ChemBioChem 7 (2006) 1783.
- [22] S. Mori, H.G. Barth, Size Exclusion Chromatography, Springer, 1999.
- [23] M. Schimpf, K. Caldwell, J.C. Giddings, Field-Flow Fractionation Handbook, Wiley Interscience, New York, 2000.
- [24] K.G. Wahlund, J.C. Giddings, Anal. Chem. 59 (1987) 1332.
- [25] C.J. Giddings, Science 260 (1993) 1456.
- [26] P.J. Wyatt, J. Colloid Interface Sci. 197 (1998) 9.
- [27] S. Tadjiki, Postnova.com.
- [28] S. Kawano, H. Murata, H. Mikami, K. Mukaibatake, H. Waki, Rapid. Commun. Mass. Spectrom. 20 (2006) 2783.
- [29] M. Leeman, K.G. Wahlund, B. Wittgren, J. Chromatogr. A 1134 (2006) 236.
- [30] P.S. Williams, J.C. Giddings, Anal. Chem. 66 (1994) 4215.
- [31] M.E. Hansen, J.C. Giddings, Anal. Chem. 61 (1989) 811.
- [32] Y. Mori, K. Kimura, M. Tanigaki, Anal. Chem. 62 (1990) 2688.
- [33] M. Pontie, X. Chasseray, D. Lemordant, J.M. Laine, J. Membr. Sci. 129 (1997) 125.
- [34] K. Stakne, M.S. Smole, K.S. Kleinschek, A. Jaroschuk, V. Ribitsch, J. Mater. Sci. 38 (2004) 2167.
- [35] J. Nagel, M. Bräuer, B. Hupfer, K. Grundke, S. Schwarz, D. Lehmann, J Appl. Polym. Sci. 93 (3) (2004) 1186.